A NUMERICAL MODEL FOR UNBOUNDED SOIL DOMAIN IN EARTHQUAKE SSI ANALYSIS USING PERIODIC INFINITE ELEMENTS

M.H.Bagheripour[1], S.M.Marandi[2]

1. Assist. Prof., Civil Engng. Dept., Shahid Bahonar University of Kerman, Iran.
E-mail: bagheri@mail.uk.ac.ir

2.Assist. Prof., Civil Engng. Dept., Shahid Bahonar University of Kerman, Iran.
E-mail:marandi@mail.uk.ac.ir

Abstract: *A rational approach is introduced for numerical modeling of unbounded soil foundations based on coupled dynamic periodic infinite and conventional finite elements (IFE-FE). The model can be applied for analysis of various dynamic problems in geomechanics, especially in Soil Structure Interaction (SSI), where determination of stiffness properties and response of unbounded soil domains are of prime importance. In numerical SSI analysis, there exists important problems; a) the discretization of natural soil foundation, especially defining the boundaries to prevent reflecting body waves and avoiding spurious results, b) the definition of the matrices related to the soil's impedance functions which are essentially dependant on the excitation frequency, c) the evaluation of free field motion of the natural foundation, especially those of irregular geometry and material diversity. An efficient way and integrated solution to these important problems is found to be the use of periodic infinite elements.*

The wave equation of motion is derived numerically for discretization of the soil domain. Shape functions and mapping coordinates for dynamic periodic infinite elements are presented in this paper. The accuracy of the IFE is examined for the evaluation of free field motion of a visco-elastic soil foundation. Derivation of impedance function is shown and leads to the determination of dynamic stiffness characteristics of the unbounded soil medium including spring and dashpot coefficients. Application of the approach introduced here is shown by analysis of SSI for a semi-tall building subjected to earthquake loading. Other advantages of the approach are the substantial reduction in degrees of freedom involved in numerical SSI analysis, the computational time and costs without sacrificing the accuracy of the results.

1-Introduction

In general, natural soil foundations have the characteristics of geometrical irregularity and boundary infinite extension as well as the complexity and diversity in material behavior. To obtain a numerical solution for such foundations in geomechanics, especially in an SSI analysis, it is necessary to describe a domain of infinite extent in a way that the soil or rock mass is assumed to be infinitely large. It is possible to use a large number of finite elements(FE) extending to a distance far enough away from the area of loading such that the truncated boundaries of the FE mesh do not influence the result. However, this requires a large amount of computational effort and computer storage. Consequently, the accuracy of the results largely depend on the type, the location of the boundary from the area of disturbance, and the number of finite elements employed in the analysis. The arbitrary location of the boundaries may result in significant error in the solution[1]. Therefore, the location of the boundary is most often selected by use of trial and error to achieve an acceptable degree of accuracy. This means the use of extra computational time again.

More importantly, numerical analysis of dynamic, earthquake, and wave propagation problems in geomechanics presents additional difficulties; First, the reflection of the body waves form the truncated and fixed boundaries are reported to cause spurious results in the past studies[2]. To overcome this problem, a vast variety of artificial finite

boundaries and coupling techniques are introduced in the literature. Among these, the viscous boundary by Lysmer & Kuhlmeyer [3] and the wave transmitting boundary by Liao et al. [4], coupling techniques with boundary elements by Wolf [5] and also by Beer [6] are mentioned here. A comprehensive review on all these solution concepts show that, they have advantages and/or disadvantages and lack of generality in application. Second, dynamic stiffness properties of the soil foundations are essentially dependant on the exciting or loading frequency. Therefore, frequency domain analysis is the only approach to determine these properties and to evaluate the matrices relating to the impedance function of the soil layer.

In this paper, a special technique is adopted for the numerical modeling of the unbounded soil medium using coupled IFE-FE technique and is used subsequently in substructure SSI analysis. As shown in Figure (1), the whole soil domain considered is divided into two sub domains namely near field (interior domain) and far field (exterior domain). The former includes the structure and possibly a limited part of the soil foundation (depending on the type of structure resting on the soil) which is modeled by conventional finite elements whereas the latter comprises the rest of the soil foundation which extends to infinity and is modeled by infinite elements. The technique introduced here enables one to efficiently evaluate the soil dynamic impedance by degenerating the equation of motion for the whole system into the near and the far fields and solving for the far field modeled by periodic infinite elements. The accuracy of the periodic infinite elements is evaluated and verified through the analysis of site response and free field motion of the soil foundation as well as the comparison of results with those obtained by available

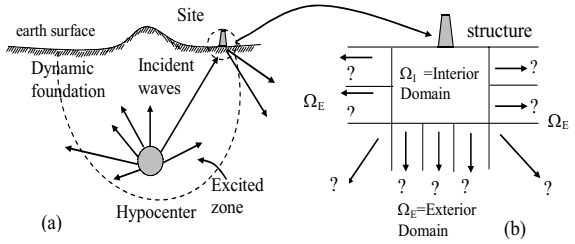

Figure 1: (a): propagation of body waves ; (b) global discretization of the whole soil domain to Interior and Exterior Domains

analytical transfer functions. A computer program has been developed based upon the dynamic IFE-FE coupling technique which allows the numerical analysis of unbounded soil in frequency domain. To complete the SSI analysis and recover the response of the structure in time domain, the analysis process can be linked to any available structural FE software. An alternative analysis can be performed using Fast Fourier Transform (FFT) and its inverse process (IFFT) [7,8,9]. In summary, time domain SSI analysis by the current approach can be performed more easily using a less computational time and memory due to the fact that the model reduces the number of degrees of freedom in the system while keeping acceptable degree of the results accuracy.

Example of SSI analysis based on the concept introduced here is presented for a 10-storey building subjected to earthquake loading. Discussion, and comparison of the results obtained continues throughout the paper.

2-Wave Equation Discretization in a Visco-Elastic Foundations

Figure (1a) depicts the propagation of earthquake waves from the hypocenter to reach the area of interest. Considering the fact that the earthquake load can be decoupled into a series of harmonic loads having different frequencies [5,18], it is assumed that the foundation is subjected to such a harmonic load. If the medium possesses constant hysteretic damping, the

governing equation of the wave motion can be written as:

$$G^*\left(\frac{\partial^2 U}{\partial x^2}+\frac{\partial^2 U}{\partial y^2}\right)+\left(\lambda^*+G^*\right)\left(\frac{\partial^2 U}{\partial x^2}+\frac{\partial^2 V}{\partial x\partial y}\right)+f_x=\rho\ddot{U}$$

$$G^*\left(\frac{\partial^2 V}{\partial x^2}+\frac{\partial^2 V}{\partial y^2}\right)+\left(\lambda^*+G^*\right)\left(\frac{\partial^2 U}{\partial x\partial y}+\frac{\partial^2 V}{\partial y^2}\right)+f_y=\rho\ddot{V}$$

$$G^*=G(1+i\eta_d)\qquad \lambda^*=\lambda(1+i\eta_d)$$

(1a,b,c)

where $U\&V$ are particle displacements in a plane domain, G is the shear modulus, λ is the Lame's constant, η_d is the viscous coefficient, and f_x, f_y are the unit body forces. Rearranging Eq.(1) leads to:

$$\frac{\partial}{\partial x}\left(D_{11}^*\frac{\partial U}{\partial x}+D_{12}^*\frac{\partial V}{\partial y}\right)+D_{33}^*\frac{\partial}{\partial y}\left(\frac{\partial U}{\partial y}+\frac{\partial V}{\partial x}\right)+fx-\rho\ddot{U}=0$$

$$D_{33}^*\frac{\partial}{\partial x}\left(\frac{\partial U}{\partial y}+\frac{\partial V}{\partial x}\right)+\frac{\partial}{\partial y}\left(D_{12}^*\frac{\partial U}{\partial x}+D_{22}^*\frac{\partial V}{\partial y}\right)+fy-\rho\ddot{V}=0$$

(2a,b)

in which D^*_{ij} $(i,j=1,2,3)$ are elements of the complex constitutive matrix $[D^*]$ and has the following form for plane strain problems:

$$[D^*]=\frac{E(1+i\eta_d)}{1+\mu}\begin{bmatrix}\frac{1-\mu}{1-2\mu} & \frac{\mu}{1-2\mu} & 0\\ \frac{\mu}{1-2\mu} & \frac{1-\mu}{1-2\mu} & 0\\ 0 & 0 & \frac{1}{2}\end{bmatrix} \qquad (3)$$

where E and μ are modulus of elasticity and Poison's ratio respectively. For any discretized element, the general weighting residual method is applied and yields to:

$$\iint_A T_1\left[\frac{\partial}{\partial x}\left(D_{11}^*\frac{\partial U}{\partial x}+D_{12}^*\frac{\partial V}{\partial y}\right)+D_{33}^*\frac{\partial}{\partial y}\left(\frac{\partial U}{\partial y}+\frac{\partial V}{\partial x}\right)+fx-\rho\ddot{U}\right]dA=0$$

$$\iint_A T_2\left[D_{33}^*\frac{\partial}{\partial x}\left(\frac{\partial U}{\partial y}+\frac{\partial V}{\partial x}\right)+\frac{\partial}{\partial y}\left(D_{12}^*\frac{\partial U}{\partial x}+D_{22}^*\frac{\partial V}{\partial y}\right)+fy-\rho\ddot{V}\right]dA=0 \qquad (4a,b)$$

in which T_1 and T_2 are weighting functions and A is the element area. If the boundary conditions are introduced, then by integrating by parts we obtain[2]:

$$\iint_A\left[\frac{\partial T_1}{\partial x}\left(D_{11}^*\frac{\partial U}{\partial x}+D_{12}^*\frac{\partial V}{\partial y}\right)+D_{33}^*\frac{\partial T_1}{\partial y}\left(\frac{\partial U}{\partial y}+\frac{\partial V}{\partial x}\right)+T_1\rho\ddot{U}-T_1f_x\right]dA-\int_{Se}T_1\overline{X}dS=0$$

$$\iint_A\left[D_{33}^*\frac{\partial T_2}{\partial x}\left(\frac{\partial U}{\partial y}+\frac{\partial V}{\partial x}\right)+\frac{\partial T_2}{\partial y}\left(D_{12}^*\frac{\partial U}{\partial x}+D_{22}^*\frac{\partial V}{\partial y}\right)+T_2\rho\ddot{V}-T_2f_y\right]dA-\int_{Se}T_2\overline{Y}dS=0 \qquad (5a,b)$$

where $\overline{X},\overline{Y}$ are the surface boundary tractions. Displacements within the element are approximated as follows:

$$\begin{Bmatrix}U\\ V\end{Bmatrix}=[N]\{u\} \qquad (6)$$

in which $[N]$ is the shape function matrix; while $\{u\}$ is the nodal displacement vector. Using Galerkin weighting functions, we have $T_{1i}=T_{2i}=N_i$ and $(i=1,2,....n)$ in which n is the number of element nodes.

2-1 Dynamic and Frequency Dependant Finite Elements(FE) Formulation

The discretized equation of wave motion can be obtained using Galerkin weighted residual procedure and ignoring body forces in Eqs. (5) to (6) which yields

$$-\omega^2[M]\{u\}+(1+i\eta_d)[K]\{u\}=\{F_\circ\} \qquad (7)$$

where $\{u\}$ is the unknown nodal displacement vector, ω is the exciting frequency, $[M]$ and $[K]$ are global mass and stiffness matrices of the system respectively and $\{F_o\}$ is the amplitude vector of the applied harmonic load. These matrices and vectors can be assembled from the element sub matrices and sub vectors which have the following forms:

$$[M]^e=\iint_A [N]^T \rho[N]dA \ \&$$
$$[K]^e=\iint_A [B]^T [D^*][B]dA \ \& \quad (8)$$
$$\{F_\circ\}^e=\int_{Se} [N]^T \{\overline{X_\circ}\}ds$$

in which $\overline{X}_o$ is the amplitude vector of boundary traction; ρ is the material density. If the viscous coefficient η_d in Eq. (7) is zero, it will degenerate to the linear elastic undamped one. Considering the fact that $[c]=\eta_d/\omega[K]$, then Eq. (7) can be rewritten as:

$$\left[-\omega^2[M]+i\omega[C]+[K]\right]\{u\}=\{F_o\} \quad (9)$$

Both of Eqs. (7) and (9) can be regarded as the equation of motion in frequency domain which will be used subsequently in the following sections where the soil dynamic impedance function and related matrices are derived.

2-2Dynamic Periodic Infinite Elements (IFE)

Ungless [10] was apparently the first to introduce the formulation of the static type of infinite element. For dynamic problems, however, Chow & Smith[11] and Zhao& Valliappan[12] and Zhao & Zhang [13] were those who introduced and apply the dynamic infinite elements in various geomechanical problems. A comprehensive review on the types and the formulation of both the static and dynamic infinite elements is found in [14]. More recently Kim & Yun [15] have applied infinite elements to the SSI analysis of a block foundation vibration.

The main advantages of using infinite elements are clearly saving of computer time and storage as well as cost reduction without sacrificing the accuracy of the solution. Furthermore, the infinite elements have all the advantages of conventional finite elements and allow such features as a banded stiffness matrix and numerical integration procedures to be retained. In summary, all numerical results indicate that, the coupling technique of finite element and infinite elements(IFE-FE) is a powerful method to simulate dynamic foundations and wave propagation problems in infinite media. Since the dynamic characteristics of the soil medium are essentially frequency dependant, the periodic (so called frequency dependant) infinite elements are of prime consideration in an SSI study. In the following, a summary of the dynamic periodic infinite elements is presented. In formulation of these infinite elements for dynamic problems, amplitude decay and phase delay of wave propagation have to be taken into account; thus, complex displacement shape functions need to be considered. The shape function of the periodic infinite element must reflect the characteristics of the far field i.e it must satisfy the radiation condition as well as the decay of the state variables (e.g. displacements) to zero at infinity. The shape function for an infinite element extending to infinity in the ζ direction may be written as:

$$N'_j(\xi,\eta)=N_j(\xi,\eta)e^{-ik\xi}e^{(\xi_1-\xi)/L} \quad (10)$$

Where $N_j(\xi,\eta)$ is the conventional element shape function, k is wave number of propagating wave and L is the scaling length. The first exponential term in Eq.(10) represents the basic shape of the propagating wave while the second exponential term enables the variables to decay to zero at infinity. A detailed discussion on the effect of the scaling length L can be seen in other published works (e.g. in [11]) . The element matrices are formulated in the usual way. The element stiffness and mass matrices are expressed of the form:

$$\int_0^\infty \int_{-1}^{+1} f(\xi,\eta)e^{-(\alpha+i\beta)\xi}d\eta d\xi \quad (11)$$

where ζ and η are the local coordinates of

the quadrilaterals. The Gauss-legendre numerical integration scheme is used in the direction not extending to infinity. Newton-Cots integration scheme, originally devised by Bettes and Zienkiewicz is used for the direction extending to infinity as follows[21]:

$$\int_0^{\infty} f(\xi)e^{-(\alpha+i\beta)\xi}d\xi \cong \sum_{s=1}^{n+1} W_s f(\xi_s) \qquad (12)$$

The number of the sampling points required will depend on the conventional element shape function given in Eq.(12) but they may be chosen as proportional to the wave length of the propagating wave or arbitrary taken at predefined points[11]. The existence of the multiple wave types in periodic elasticity problems would make the latter option more efficient. The weighting coefficients are given as :

$$W_s = \int_0^{\infty} A_s e^{-(\alpha+i\beta)\xi}d\xi \qquad \text{and} \qquad (13)$$

$$A_s = \prod_{\substack{j=1 \\ \neq s}}^{n+1} \left(\frac{\xi_j - \xi}{\xi_j - \xi_s} \right) \qquad (14)$$

A)Transformation of Element Coordinates in a Plane Domain

Consider the infinite element shown in Figure (2), transformation of the element coordinates are[2,14,16]:

$$x = \sum_{i=1}^{5} N_i' x_i \qquad y = \sum_{i=1}^{5} N_i' \qquad (15)$$

where $N_i'(i = 1,2,...,5)$ is the mapping function of the infinite element and can be expressed as:

$$N_1' = \frac{1}{2}(\xi - 1)(\eta - 1) \quad N_2' = 0 \quad N_3' = \frac{-1}{2}(\xi - 1)(\eta + 1)$$
$$N_4' = \frac{1}{2}\xi(\eta + 1) \quad N_5' = \frac{-1}{2}\xi(\eta - 1) \qquad (16)$$

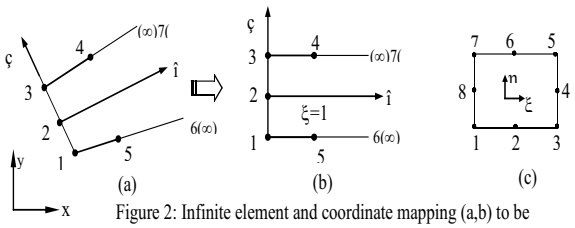

Figure 2: Infinite element and coordinate mapping (a,b) to be connected to conventional finite element(c)

B)Displacement Shape Function of Element

For the case when coupling with 3 to 8 node isoparametric finite elements (Figure 2b,c), the following displacement shape functions are employed:

$$u = \sum_{i=1}^{3} N_i u_i \quad v = \sum_{i=1}^{3} N_i v_i \qquad \text{and} \qquad (17)$$

$$N_1 = \mathrm{P}(\xi)\frac{\eta(\eta - 1)}{2}$$
$$N_2 = -\mathrm{P}(\xi)(\eta - 1)(\eta + 1) \qquad (18)$$
$$N_3 = \mathrm{P}(\xi)\frac{\eta(\eta + 1)}{2}$$

in the above equations $P(\zeta)$ is the propagation function. Based on the discussion given for 1-D problems, the propagation function can be written as[2,16]:

$$P(\xi) = e^{-(\alpha + i\beta)\xi} \qquad (19)$$

where α and β are the displacement amplitude decay factor and nominal wave number in the local coordinates of infinite elements respectively. The term $e^{-\alpha\zeta}$ expresses the amplitude attenuation due to wave dispersion while $e^{-i\beta\zeta}$ defines the phase delay due to wave propagation in the local coordinate system. Considering Figure (3) transformation of element coordinates requires that:

$$\xi = \frac{X - X_1}{X_2 - X_1} \qquad (20)$$

Hence the Eq. (19) may be written as:

$$P(X) = \exp\left[-\left(\frac{\alpha}{l(X_2)} + i\frac{\beta}{l(X_2)} \right)(X - X_1) \right] \qquad (21)$$

where X_1 and X_2 are the global coordinates of points 1 and 2 in figure (3); $l(X_2)=X_2-X_1$ is the distance between nodes 1 and 2 which is a function of X_2 when X_1 is fixed. The same principle applies in treating a 2-D plane domain problems ,however, it needs a lengthy discussion which is beyond the scope of this paper and are presented elsewhere (e.g. in [2]).

2-3 Mass and Stiffness Matrices and Numerical Integrations for IFE

With reference to finite element formulation and wave propagation behavior, the mass and stiffness matrix for infinite elements can be written as:

$$[M]^e = \int_{-1}^{1} \int_{0}^{\infty} [N]^T \rho [N] |J| d\xi . d\eta \qquad (22\ a,b)$$

$$[K]^e = \int_{-1}^{1} \int_{0}^{\infty} [B]^T [D^*] [B] |J| d\xi . d\eta$$

In which lJ is the Jacobian determinant. From Eq. (22) calculations of the infinite element matrix need to consider a generalized integrals of the form:

$$I = \int_0^{\infty} F(\xi) \exp\left[-2(\alpha^* + i\beta^*)\xi \right] d\xi \qquad (23)$$

where $\alpha^* \sim \alpha + 1/2.\eta_d.\beta$ and $\beta^* \sim \beta = \omega/C$ in which C is the shear wave velocity in the material. The condition $\alpha^* > 0$ is sufficient for convergence of Eq. (23). A physical meaning for this condition is that wave propagation is always accompanied by dispersion attenuation. The selection of integration points and weighting coefficients are lengthy to be discussed and interested readers are referred to[2].

2-4 Program DYNINF

A computer program called DYNINF has been developed by authors for 2-D numerical modeling of dynamic, earthquake and wave propagation problems in geomechanics. The program has been used for other studies(e.g. in[9]). Dynamic and conventional finite elements are developed based on Eq. (9) and are assembled in conjunction with dynamic infinite elements (Eqs.15-23) to make an assemblage of near and far field of the problem respectively.

The program has been written using Fortran 90 codes of programming and, at this stage, has no complementary parts such as preprocessing and/or post processing. Another version of the program for 3-D dynamic problems has also been developed by first author and could be used for SSI analyses [16].

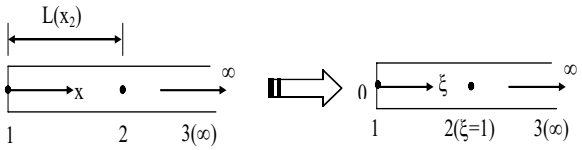

Figure 3: mapping coordinates for a 1 -D infinite element.

3-Substructuring SSI Concept

Usually in sub structuring SSI analysis the whole system is broken down into separate parts as shown in Figure (4A). According to this, two main steps in substructure concept for SSI analysis are: 1) determination of free field motion(Figure 4B) under a given base strong motion and 2) Evaluation of dynamic impedance and stiffness coefficient of soil foundation which are essentially frequency dependant. In such a general concept, the dynamic stiffness coefficients of the soil can physically be interpreted as a generalized spring-dashpot system. Thus, SSI analysis is carried out for the structure supported on these spring-dashpot system (Figure 4C) and for a loading case which depends on the free field motion[9]. Assuming a linear behavior for the system, superposition principle governs the equations of motion for the soil

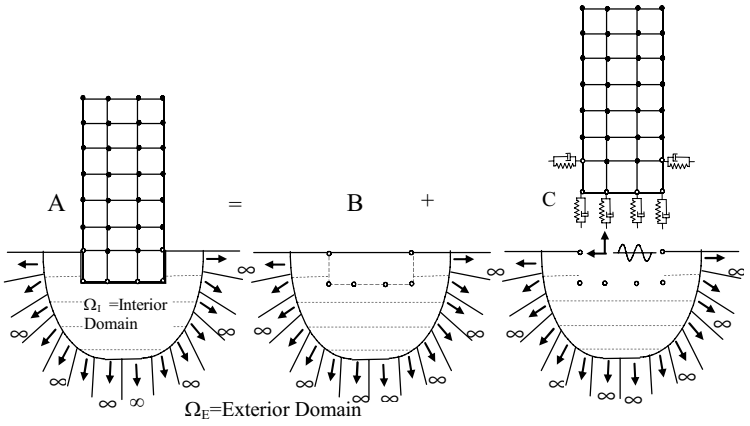

Figure 4: Dynamic foundation discretized to Exterior and Interior domains

and the structure and hence the substructure concept allows breaking the whole system into more manageable parts which can be easily analyzed [5].

3-1 Model Formulation for Dynamic Impedance Matrix of Unbounded Soil

The equation of motion for the whole system shown in Figure (4A) can be expressed as [17]:

$$[M_t]\{\ddot{u}\}+[C_t]\{\dot{u}\}+[K_t]\{u\}=\{P\} \qquad (24)$$

Where $[M_t]$,$[C_t]$, and $[K_t]$ are the total mass, damping, and stiffness matrices while $\{P\}$ is the vector of exciting force. These matrices are further defined as:

$$\begin{aligned}[M_t]&=[M_n]+[M_f]\\ [C_t]&=[C_n]+[C_f]\\ [K_t]&=[K_n]+[K_f]\end{aligned} \qquad (25a,b,c)$$

The subscripts *n* and *f* represent the near and far field respectively. The vectors $\{u\}$,$\{u'\}$,and $\{u''\}$ represent the displacement, velocity , and acceleration vectors respectively. Eq. (24) is, in fact, a restatement of the equation of motion (i.e.Eq.9) in time domain when the frequency to time domain transformations are considered:

$$\begin{aligned}\dot{u}&=i.\omega.u_\circ \exp i\omega t\ , \quad \ddot{u}=-u_\circ.\omega^2 \exp i\omega t\\ u&=u_\circ \exp i\omega t\ , \quad p=F_\circ \exp i\omega t\end{aligned} \qquad (26)$$

where *u',u"*are the particle velocity and acceleration respectively. If the far field is modeled by infinite elements (Figure 5) for a given frequency, say ω, the decoupled equation of motion for only the far field is defined as in Eq. (9):

$$\left[-\omega^2[M_f]+i\omega[C_f]+[K_f]\right]\{u_f(\omega)\}=\{p_f(\omega)\}$$
$$\left[\overline{K_f(\omega)}\right]\{u_f(\omega)\}=\{p_f(\omega)\} \quad \text{or} \qquad (27a,b)$$

considering the fact that, the system is analyzed in frequency domain and that in such solutions the displacements and forces are of a complex form, thus;

$$\{u_f(\omega)\}=u_1+i.u_2 \quad and \quad \{p_f(\omega)\}=p_1+i.p_2 \qquad (28)$$

for any harmonic excitation, the load –displacement relation is again defined in a complex form as:

$$\left[\overline{K_f(\omega)}\right]=[K_1(\omega)]+i.[K_2(\omega)]=\frac{\{p_f(\omega)\}}{\{u_f(\omega)\}} \qquad (29)$$

in which $\left[\overline{K_f(\omega)}\right]$ is, in fact, the dynamic impedance matrix of the far field of the system. It is seen that both the $[K_1\omega]$ and $[K_2\omega]$ are functions of the exciting frequency which constitute imaginary parts of the total stiffness matrix respectively. They define the stiffness and the damping characteristics of the soil medium. Assuming

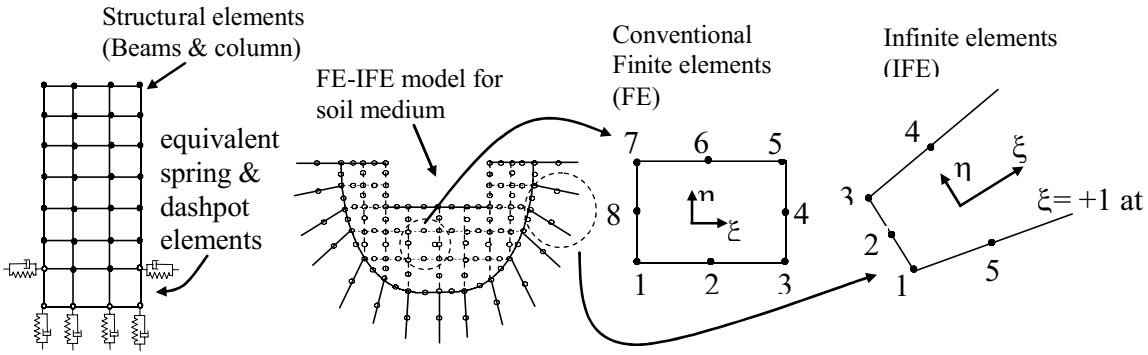

Figure 5: Finite and Infinite element (FE -IFE) model for the soil and the structure supported on fictitious generalized springs and dashpots

the frequency ω_S is a constant coefficient in the analysis, the soil system shown in Figure (5) can be represented by a set of fictitious generalized spring-dashpot system. They virtually reflect the coupling effects among the node in the common side between the near field (i.e. the structure) and the far field of the system. From Eqs. (27) to (29), these matrices can be rewritten in the following forms:

$$\left[\mathrm{Re}[\overline{K_f(\omega_s)}]\right]=\left[K_1(\omega_s)\right]=$$
$$\left[-\omega_s^2\left[\mathrm{Re}[M_f(\omega)]\right]-\omega_s\left[\mathrm{Im}[C_f(\omega)]\right]+\left[\mathrm{Re}[K_f(\omega)]\right]\right]$$
$$\left[\mathrm{Im}[\overline{K_f(\omega_s)}]\right]=\left[K_2(\omega_s)\right]=$$
$$\left[-\omega_s^2\left[\mathrm{Im}[M_f(\omega_s)]\right]+\omega_s\left[\mathrm{Re}[C_f(\omega_s)]\right]+\left[\mathrm{Im}[K_f(\omega_s)]\right]\right]$$

(30 a,b)

in the above equations, the abbreviations Re and *Im* denote the real and imaginary parts of the matrices respectively. ω_S is the resonant frequency of the system , M_f, C_f, and K_f are the representative mass, damping, and stiffness characteristics of the far field while K_1 and K_2 are the absolute values of the real and imaginary part of the stiffness coefficient.

The total equivalent stiffness matrix of all fictitious generalized spring $[K_f]_e$ and the equivalent damping matrix of all fictitious generalized dashpots $[C_f]_e$ in the system can be defined as:

$$\left[K_f\right]_e=\left[K_1(\omega_s)\right] \quad \left[C_f\right]_e=1/\omega\left[K_2(\omega_s)\right] \quad (31)$$

The discretized equation of motion for the whole system can now be reassembled as follows:

$$\left[M_n\right]\{\ddot{u}\}+\left(\left[C_n\right]+\left[C_f\right]_e\right)\{\dot{u}\}+$$
$$\left(\left[K_n\right]+\left[K_f\right]_e\right)\{u\}=\{P\} \quad (32)$$

The matrix $[M_f]$ is no longer involved in Eq. (32) since the infinite descretized soil domain has now be replaced by a set of massless spring-dashpots (Figure 5) at the connecting nodes between the structure and the soil medium.

The significance of the proposed method here reveals that : 1) the Eq. (32) is rigorous in time domain provided the matrices $[K_f]_e$ and $[C_f]_e$ are rigorous in the equation; and 2) large number of degrees of freedom related to the discretized and infinite soil domain have now been much reduced to only limited degrees of freedom related to generalized fictitious springs and dashpots. The accuracy of the solution from Eq. (32) to some extent depends on the frequency ω_S. For an SSI system or a layered soil foundation, however, there exists fundamental or resonant frequencies in the soil layer or in the structure. It appears logical to select ω_S as close as possible to these frequencies.

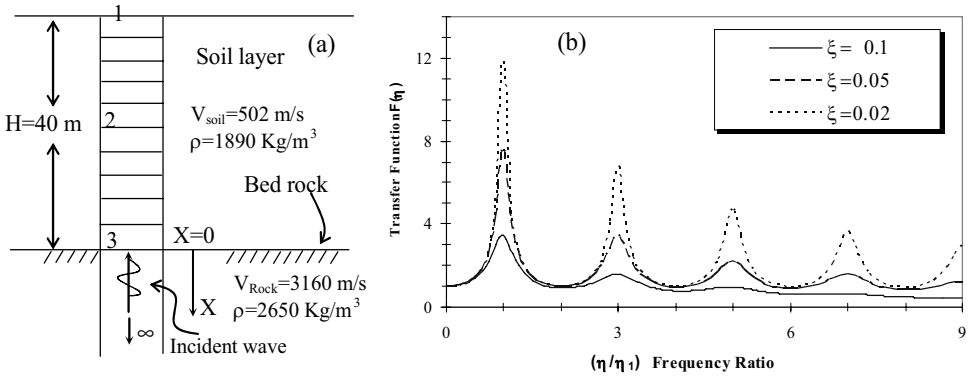

Figure 6: (a) Soil layer overlaying bedrock, and (b) transf er function values for the soil layer

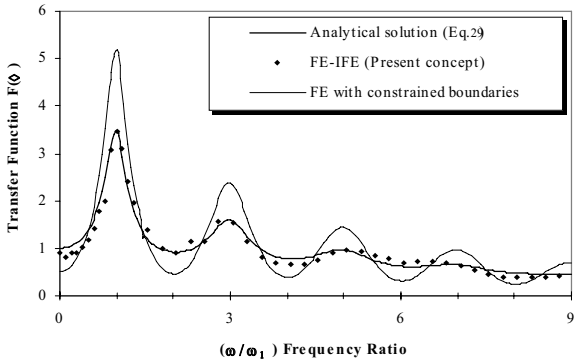

Figure 7: Comparison of results obtained for free response of the soil layer

Assuming ω_S is constant throughout the SSI analysis, the periodic infinite elements and their virtual substitutes (i.e. spring and dashpots) become independent of the loading frequency. Therefore, Eq. (32) can now be solved by other conventional FE program in time domain using a reduced number of degrees of freedom.

3-2 Site Response and Verification of the Accuracy of the Infinite Elements

In order to investigate the accuracy of the present concept in SSI analysis, a soil layer overlaying the sound rock formation has been analyzed. As shown in Figure (6a) and assuming a unit harmonic acceleration wave vertically propagates from the rock formation through the soil layer, the analytical solution of the problem can be expressed in the form of transfer function as[18,19]:

$$F(\omega) = 1/\{\cos[\omega H / V_1(1+i\xi)] + i.K \sin[\omega H / V_2(1+i\xi)]\} \quad (33)$$

In the above equation, $F(\omega)$ is the transfer function, ω is the exciting frequency, V_1 and V_2 are the shear wave velocities in the soil layer and rock formation respectively, H is the thickness of the soil layer, ζ is the damping coefficient in the soil and finally K is the impedance ratio defined by:

$$K = \frac{\rho_1 V_1}{\rho_2 V_2} \quad (34)$$

in which ρ_1 and ρ_2 are the density of the soil layer and rock formation respectively. The soil layer has fundamental natural frequency as $\omega_1=\pi V_1/2H$. Eq. (33) is derived based on the assumption that, all boundaries are horizontal and that the response of the soil deposit predominantly caused by *SH* waves

propagating vertically from underlying bedrock. The surface of soil and rock are also assumed to extend infinitely in the horizontal direction. Procedures based on this assumptions have shown to predict ground response that is in reasonable agreement with measured response in many cases [18]. The values for the transfer function can be viewed as the magnification factors to be multiplied by the unit input displacements to reach the displacements at the surface of soil layer. Figure (6b) shows the analytical solution of site response and the transfer function values obtained in the selected soil layer for three different damping coefficients (ζ=0.1, 0.05, 0.02). It is seen from the figure that as the excitation frequency approaches the natural frequencies of the soil layer (i.e. ω/ω_1=1,3,…), then magnification factor increases dramatically. While the damping coefficient increases, the magnification factors reduce especially in the higher frequency range of exciting load where transfer function values drop even below unity.

Periodic infinite elements are used to evaluate the transfer function values. Figure (7) shows the results obtained from IFE-FE modeling and those obtained by Eq. (33) for only a selected value of damping coefficient (ζ=0.1). To further show the significance of the boundary condition and the impact of the truncated boundaries in conventional finite element modeling, the same problem is analyzed by available FE software (ANSYS) using fixed boundaries. Figure (7) also shows a relatively good agreement between the results obtained from the analytical transfer function (Eq. 33) and those obtained by periodic infinite element. Clearly, this verifies the accuracy of the infinite elements in modeling of the infinite soil domains. Furthermore, since the transfer function is dependant on the stiffness and damping characteristics of the soil layer the agreement of the results also verifies the accurate and efficient evaluation of these characteristics by IFE-FE model. The agreement of the results also shows that IFE-FE model is able to capture reasonably the fundamental and main characteristics of the infinite soil domains(i.e. resonant conditions as depicted in Figure 7). On the other hand, the results obtained by conventional FE modeling (i.e. fixed or truncated boundaries) presents significant deviations from the two conforming methods mentioned above (Figure 7) and, thus, they can not be considered as reliable. Further discussion on accuracy of the infinite elements will be presented in next section where, in an example, a transient earthquake loading is applied to the bed rock and free field response motion at the surface is recovered.

4-Numerical Example of SSI Based on the Current Concept

A numerical example is investigated in this

Table 1: Structural and foundation properties adopted in the numerical example

Structural properties					**Foundation properties**			
Element	**beams**	**columns**			**proprty**	**concrete**	**soil**	**Bed rock**
properties	2IPE240	BOX(1)	BOX(2)	BOX(3)	**H**(m)	0.8	40	-
I_x=I_y (cm^4)	7780	19143	10812	7566	ρ(t/m^3)	2.4	1.89	2.65
A (cm^2)	28.6	138.27	114.24	77.44	**Vs**(m/s)	2050	502	3160
H(cm)	24	30	25	25	**E**(kN/m^2)	24E6	3.3E5	29.2E6
γ(kN/m^3)	78.5	78.5	78.5	78.5	ξ	0.02	0.05	0.02
E(kN/m^2)	20.4 E6	20.4 E6	20.4 E6	20.4 E6	Comment:Box(1)=30×30×1.2,			
ξ	0.02	0.02	0.02	0.02	Box(2)=25×25×1.2,Box(3)=25×25×0.8(cm)			

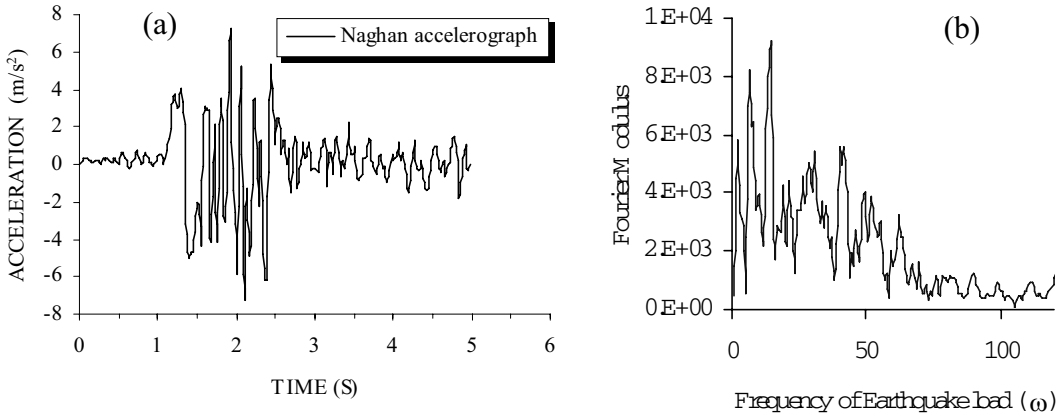

Figure 8: (a) Input acceleration time history; (b) Fourier spectrum

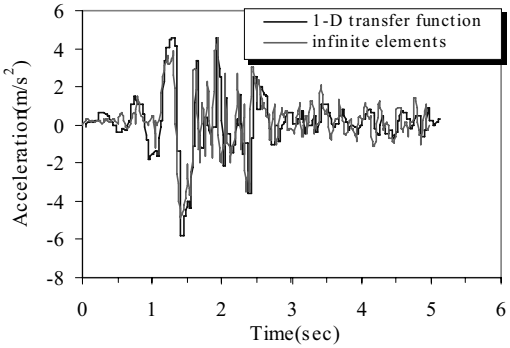

Table 2: Coefficients of the springs and dashpots obtained by FE -IFE technique

property	direction	horizontal	vertical
Ke(kN/m)		113.5E3	165.8E3
Ce(kN.Sec/m)		37E-2	38E-3

Figure 9: acceleration at soil surface obtained by FE -IFE & analytical approach

section in order to show the applicability and the efficiency of the approach adopted in this paper. Linear dynamic response and SSI analysis of a 10 story building slightly embedded in a soil layer overlaying a rock formation is presented. The geometry of the soil layer selected is basically the same as shown in Figure (6a) and its properties are summarized in table(1) in conjunction with the geometrical characteristics of the structural elements. The total height and width of the building are 32m and 12m respectively. The system under study including the soil layer and the structure is subjected to an acceleration time history of Naghan earthquake recorded in the past. The main stages of SSI analysis related to the free field response motion of the soil layer and the determination of soil dynamic impedance as well as the calculation of the generalized fictitious springs and dashpots are totally carried out in frequency domain and by means of IFE-FE technique described in preceding sections while time domain analysis is conducted by ANSYS 5.6 software. The main accelerogram for Nagan earthquake is shown in Figure (8a) while the Fourier spectrum obtained by FFT procedure (Fast Fourier Transform) is depicted in Figure (8b). Considering the fact that the soil layer beneath the structure has a thickness about 40m, then the fundamental frequency for the soil layer is evaluated as $\omega_1=\pi V_s/2H\sim19$ rad/sec which is close to the predominant frequency depicted in Fourier spectrum. The thickness of the soil layer has deliberately selected as such value (H=40) so that the soil layer exhibits its profound interaction effect under the given base strong motion (in this example Naghan earthquake record).

The response of the medium at the surface of

the soil layer is obtained next for the transient Naghan earthquake input loading. It is shown in Figure (9) which is obtained through the IFE-FE concept presented in this paper. The conventional and analytical method based on the transfer function presented in sec. 3-2 was also used to compare the results and further examine the accuracy of periodic infinite elements for transient earthquake loading. The acceleration time history of the soil layer at the surface obtained by this method is superimposed in Figure (9). As can be seen from this figure, relatively good agreement is observed between the results obtained by analytical solution and those obtained by periodic infinite elements. This again verifies the accuracy of the periodic infinite elements in evaluation of soil dynamic properties.

Interested readers may note that in case of soil medium of high geometrical irregularity and material diversity, the analytical solutions does not exists and the analysis of free field motion is possible only by a rational numerical approach such as IFE-FE concept.

Using Eq. (31), the stiffness properties of the soil foundation medium beneath the structure shown in Figure (5a) are evaluated. The total equivalent stiffness matrix of all fictitious generalized springs and dashpots in the system shown in Figure (5) are

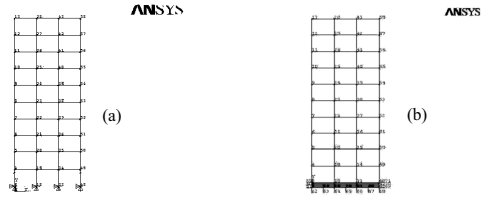

Figure 10: The structure selected in example ; (a) rigid base structure (b) structure supported by fictitious generalized springs and dashpots defined b y IFE-FE

calculated. Because of small variability, the mean values for the spring and damping coefficients obtained for common nodal points between the soil and the structure are selected and shown in Table 2. In addition, because of slight embedment for the structure, the rotational stiffness of the soil may be neglected.

4-1 Analyses Results and Discussions

Large amount of data has been obtained in the course of analysis. Presentation and discussion on all of these requires tremendous effort and time to be devoted. Only a summary on main points are presented. The linear elastic response of the structure is considered as prime importance while non-linear response analysis could be presented in separate report. A study on the maximum displacement and induced base shear force to the structure is conducted[20]. To show the interaction effect, the results are compared with those obtained in a conventional rigid base structure. In addition, the results of the current approach

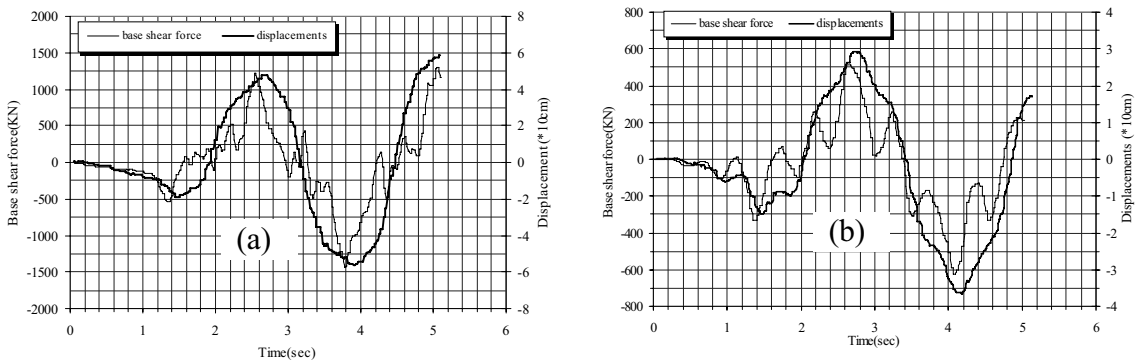

Figure 11: Max. displacemen ts and base shear forces induced to the structure in (a) conventional rigid base and (b) supported on springs & dashpots

Table 3: Comparison of the results , time, and memory obtained by 3 models

Concept	Substructure SSI (Fig 10b)	Direct SSI Approach (Fig. 12)	
Software/Program	IFE-FE +ANSYS	ANSYS	PLAXIS
Max. Displacement (cm)	31	37	36
Max. base shear force (kN)	636 kN	684 kN	701kN
Memory required (kB)	27E3	322 E3	256E3
Computational time (sec)	35	1800	1550

are further compared with those obtained in other SSI concepts such as direct method [5].

4-2 Conventional Rigid Base Structural Response

A conventional earthquake analysis for the structure shown in Figure (10a) is presented first where the effect of soil presence is not considered. In Figure (11) the variation of maximum displacement of the rigid base structure at the top for Naghan earthquake is shown. It is seen, from this figure that, the maximum displacement of rigid base structure reaches 57 cm . Also, in this figure. the variation of base shear force for the rigid base structure vs time is depicted. The figure shows that the structure undergoes a maximum base shear force of about 1.47MN.

4-3 Response of the Structure Supported on Springs and Dashpots

The structure supported on springs and dashpots (Figure 10b) is now subjected to the input motion which corresponds to the free field and response of the soil layer obtained in preceding section (Figure 9). Response of the structure is again of interest mainly for the sake of comparison and investigating the effect of soil interaction. Figure (11b) shows the variation of the maximum displacement and the base shear force with time for the structure. From this figure, it can be shown that the maximum displacement induced to the structure reached about 30 cm while the base shear force exceeds slightly 650 kN. Comparison of the results shown in Figure (11b) with those obtained for rigid base structure (Figure 11a) reveals that the maximum displacement of the structure has been reduced mainly because of the interaction effect or the action of the springs and dashpots. The spring and dashpots represent the visco-elastic soil medium which, considering the interaction effect, undergoes deformation and hence the relative deformation of the structure is reduced. In fact, both the material and geometrical dampings have been integrated in the form of connecting nodal dashpots defined by periodic infinite element concept. These dashpots contribute mostly in dissipation of earthquake energy and hence in reduction of the structural response [5].

4-4 Further Comparison of the Results with Direct SSI Approach

Further study is conducted to show the efficiency and the accuracy of the results obtained in the numerical example. Here, the results are compared with those obtained by another SSI approach namely direct method [5,7,8]. Despite the substructure method, the direct approach includes analysis of a system of soil and structure as a whole and at once. Therefore, the numerical model established by this concept, as shown in Figure (12) requires an extensive FE mesh fixed at the boundaries. In fact, such an extensive FE mesh was inevitable as minimum requirement to guarantee an acceptable degree of accuracy. Clearly, in such a model computational time and computer storage required would increase dramatically. Two conventional FE softwares, namely ANSYS 5.6 and PLAXIS are both used to create an assemblage of structure and soil medium as

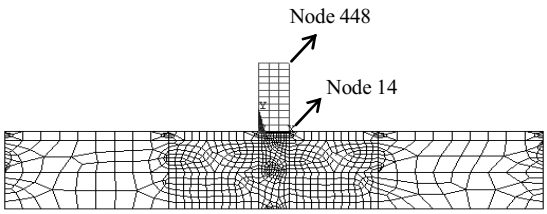

Figure 12: FE model for direct SSI analysis in structure obtained by 3 methods

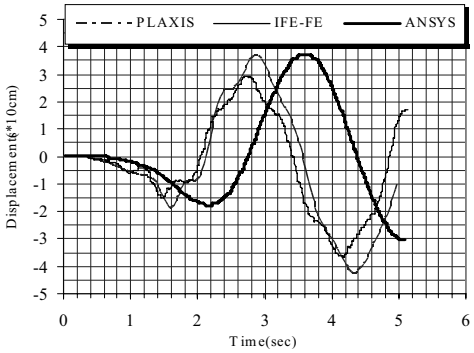

Figure 13: time history of displacement of the example using an extensive mesh

shown in Figure (12). The response of structure is again considered and is compared with those obtained by substructring concept through IFE-FE model. Comparison of the results are shown in Figure (13). It is seen, from this figure, that the structural response obtained at the top given by PLAXIS and by IFE-FE concepts ,albeit little deviation, are in reasonable agreement through the whole time span of the analysis. However, the results given by ANSYS model shows a time phase delay in response compared with the other two. Table(3) shows a summary of the results obtained by three numerical models discussed above. In the table, the computational times required by a unique computer with the same CPU used throughout the study and for all three models are also presented. Comparison of the computational times and the memory allocated by computer reveals that in the current approach based on IFE-FE , minimum time and memory is required mainly because of the large reduction of the number of degrees of freedoms related to the soil domain replaced by springs and dashpots.

5-Conclusions

A numerical method based on the coupled finite and periodic infinite elements(IFE-FE) was presented to better model the dynamic unbounded soil foundations and was applied to earthquake SSI analysis of the structures. The method divides the infinite soil domain into the near field and the far fields. The near field is modeled by finite elements coupled to the periodic infinite elements representing the rest of the foundation extending to infinity as the far field. The method is efficient in a better evaluation of the soil dynamic impedance and the determination of fictitious generalized springs and dashpots characteristics as well as the calculation of the free field motion of the soil surface. In addition, the concept presented is powerful in reducing the number of degrees of freedoms, mesh size, and hence computational time without loosing the accuracy of the results.

The accuracy of the periodic infinite elements was shown in the numerical analysis of free field response of the soil layer and in the substructure SSI analysis of a semi-tall building subjected to earthquake loading. The results showed that the response of the structure is decreased due to the soil interaction effect. The results were further compared with those obtained by the earthquake SSI analysis of the same structure based on the direct approach. It was seen that the substructuring concept based on the IFE-FE technique presents reasonable agreement with those obtained by direct SSI method. However, IFE-FE concept required less computational time and computer memory.

6-References:

[1]. Taiebat H A. Elasto-plastic analysis of static geotechnical problems with infinite elements. M.Eng.Sc Dissertation, University of Sydney, 1994.

[2]. Chuhan Z. Zhao C. Coupling method of finite and infinite elements for strip foundation wave problems. J Earthquake Eng. & Struc. Dyn. 1987: 15: 839-851.

[3]. Lysmer J, Kuhlemeyer R L. Finite dynamic model for infinite media. J Eng Mech Div. ASCE 1969: 95: 850-877.

[4]. Liao Z P, Wong H L, Yifan Y. A transmitting boundary for transient wave analysis. Scientia Sinica 1984: 27:1063-1073.

[5]. Wolf J P. Dynamic Soil Structure Interaction. Prentice Hall, Englewood Cliffs., N.J., 1985.

[6]. Beer G. Finite element- Boundary element and coupled analysis of unbounded problems in elastostatics. Int. J. Num. meth. in Eng. 1993: 19: 567-580.

[7]. Wolf J P. Soil Structure Interaction Analysis in Time Domain. Prentice Hall, Englewood Cliffs., N.J.,1988.

[8]. Wolf J P, Song C. Finite Element Modelling of Unbounded Media. Wiley: N.Y., 1996.

[9]. Bagheripour M H, Marandi S M, Shakeri J. Soil structure interaction using infinite elements. Proc. 3rd Int. Symposium on Geotechnical Engng., and soil Mechanics., 9-11 Dec. 2001 Nirou Research Center Tehran Iran.(in persian).

[10]. Ungless R F. An infinite element. M.A.Sc. Dissertation. University of British Columbia, 1973.

[11]. Chow Y K, Smith I M. Static and periodic infinite solid elements. Int. J. Numer. Meth. Engng, 1981: 17: 503-526.

[12]. Zhao C, Valliappan S. A dynamic infinite element for 3-D infinite domain wave problems. Int. J. for Numer. Meth. Engng. 1992:36:2567-2580.

[13]. Zhao C, Zhang C. Analysis of 3-D foundation wave problems by mapped dynamic infinite elements. J. Science in China, 1989: 32: 49-491.

[14]. Bagheripour M H, Marandi S M. Analysis of static and dynamic problems in geotechnics with infinite elements. proc. 6th Int. Conf. in Civil Engng. (ICCE 2003), 4-6 April, 2003 University of Technology Isfahan, Iran. (in Persian)

[15]. Kim D, Yun C. Time domain soil structure interaction analysis in two-dimensional medium based on analytical frequency dependant infinite elements. Int. J. for numer. Meth. In Engng 2000: 47: 1241-1261.

[16]. Bagheripour, M H. Earthquake response analysis of brick masonary buildings by dynamic infinite element method. M.Eng.Sc. Dissertation, University of New South Wales, Sydney , Australia 1992.

[17]. Bagheripour M H, Marandi S M. Evaluation of soil dynamic impedance in soil structure interaction analysis. Proc. 4th int. Conf. Earthquake Engng. & seismology., 12-14 May, 2003, Tehran, Iran.

[18]. Kramer S L. Geotechnical Earthquake Engineering. Prentice Hall, Upper Saddle River, N.J., 1996.(Also its translated version in Persian by Dr. Mirhosseini M & Areffi B.)

[19] Baziar M H, Ghannad Z. Principles of

Soil Dynamic with Regard to Earthquake Engineering. Iranian University of Science & Technology Press. Tehran, 2003. (in Persian).

[20]. Bagheripour M H, Mazloum R. An approximate method for soil structure interaction of semi-tall buildings. Proc. 1st National Congress on Civil Engng., NCCE 1383, 12 may,2004, Sharif University of Technology, Tehran, Iran.

[21]. Bettes P , Zienkiewicz, O C , Difraction and reflection of surface waves using finite and infinite elements . Int. J. Numerical Methods in Engng. 1977:11 No. 8, PP 1271-1290.